EUROPEAN ORGANISATION FOR NUCLEAR RESEARCH

CERN-PH-EP/2005-022

9th June 2005

The IS427 and ISOLDE Collaborations

Laser and β-NMR spectroscopy on neutron-rich magnesium isotopes

M. Kowalska[1], D. Yordanov[2], K. Blaum[1], D. Borremans[2], P. Himpe[2], P. Lievens[3], S. Mallion[2], R. Neugart[1], G. Neyens[2], N. Vermeulen[2]

[1]*Institut für Physik, Universität Mainz, D-55099 Mainz, Germany*
[2]*Instituut voor Kern- en Stralingsfysica, K.U.Leuven, B-3001 Leuven, Belgium*
[3]*Laboratorium voor Vaste-Stoffysica en Magnetisme, K.U.Leuven, B-3001 Leuven, Belgium*

Abstract

Ground state properties of neutron-rich ^{29,31}Mg have been recently measured at ISOLDE/CERN in the context of shell structure far from stability. By combining the results of β-NMR and hyperfine structure measurements unambiguous values of the nuclear spin and magnetic moment of ^{31}Mg are obtained. $I^{\pi} = 1/2^{+}$ and $\mu = -0.88355(15)\ \mu_N$ can be explained only by an intruder ground state with at least 2p-2h excitations, revealing the weakening of the $N = 20$ shell gap in this nucleus. This result plays an important role in the understanding of the mechanism and boundaries of the so called "island of inversion".

PACS: 21.10.Hw- Spin, parity, and isobaric spin; 21.10.Ky - Electromagnetic moments; 27.30.+t - 20 $\leq$ A $\leq$ 38 and 32.10.Fn - Fine and hyperfine structure

Submitted to Eur. Phys. J. A direct

TABLE I: Ground state properties of ^{29,31,33}Mg (before our measurements)

isotope	half-life	nuclear spin-parity
^{29}Mg	1.3 s	$3/2^+$
^{31}Mg	230 ms	$(3/2)^+$
^{33}Mg	90 ms	$(3/2)^+$

1 INTRODUCTION

With the advent of radioactive beam facilities the number of nuclei available for study became much larger than about 300 stable nuclei investigated before. Among the ways of gaining insight into this vast variety of nuclear systems, one is to study their ground state properties. One of the regions of special interest is the "island of inversion", comprising highly deformed neutron-rich nuclei with 10 to 12 protons and about 20 neutrons. The large deformation in this region was first suggested after mass measurement of ^{31}Na [1] and has been since then observed also by other methods in some neighbouring nuclei, such as ^{30}Ne [2], ^{30}Na [3] or ^{32}Mg [2, 4]. The shell model interprets this behaviour as a sign of weakening, or even disappearance of the $N = 20$ shell gap between the sd and fp shells. Due to this, particle-hole excitations come very low in energy and even become the ground state, giving rise to the inversion of classical shell model levels, thus the name of the region. The exact borders of this "island" are not known. Odd-A neutron-rich radioactive Mg isotopes lie on its onset, or probably even inside it. Their nuclear moments are not known and only the spin of ^{29}Mg has been firmly assigned [4], and the spins of ^{31,33}Mg have been assigned tentatively [5, 6] (Table I). It is therefore important to study these systems.

2 EXPERIMENTAL PROCEDURE AND TESTS

The beams of interest are produced at the ISOLDE mass separator at CERN via nuclear fragmentation reactions in the UC_2 target by a 1.4 GeV pulsed proton beam (about 3×10^{13}/s protons per pulse, every 2.4 seconds). They are next ionised by stepwise excitation in the resonance ionisation laser ion source [7], accelerated to 60 kV and guided to the collinear laser spectroscopy setup [8], where laser and β-NMR spectroscopy are performed (Fig. **??**). The typical ion intensities available are 6.5×10^6, 1.5×10^5, and 8.9×10^3 ions/s of ^{29}Mg$^+$, ^{31}Mg$^+$, and ^{33}Mg$^+$, respectively. In the experimental setup the ions are polarised, implanted into a crystal lattice and the angular asymmetry of their β-decay is detected [9].

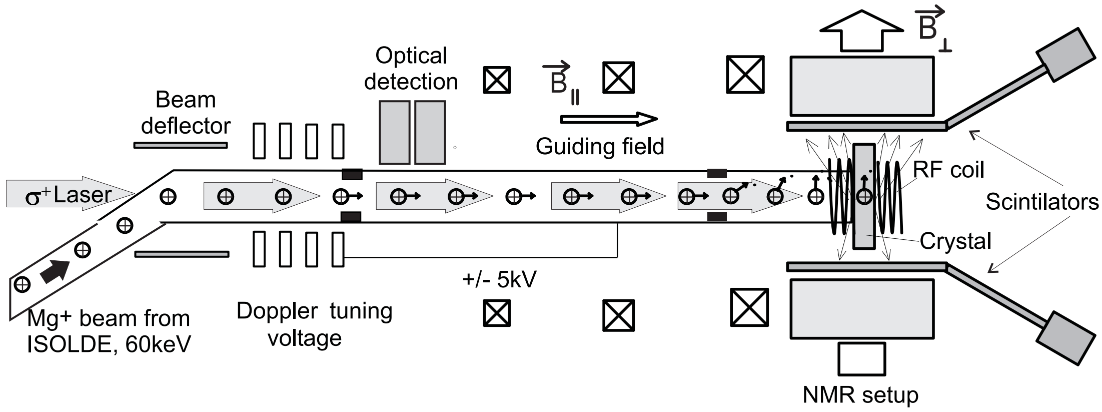

FIG. 1: Experimental setup for laser and β-NMR spectroscopy on Mg ions. For the measurements, either the optical detection, or the β-NMR is used.

The polarisation is obtained via optical pumping (see [3]). For this purpose the ions are overlapped with circularly polarised cw laser light and their total spins (electron and nuclear) get polarised due to the interaction with the light in presence of a weak longitudinal magnetic field. When positive laser polarisation is chosen (σ^+), after several excitation-decay cycles the ground state sublevel with highest m_F (projection of the total atomic spin F in the direction of the guiding magnetic field) is mostly populated. For σ^- the population is highest for the lowest $m_F = -F$ (Fig. 2). The electric and nuclear spins are next rotated in a gradually increasing guiding field and adiabatically decoupled (Fig. 3) before the ions enter the region of a high transversal magnetic field (0.3 T), where they are implanted into a suitable host crystal. With polarised spins the β-decay is anisotropic and the angular asymmetry of the emitted β particles can be measured in two detectors, placed at 0 and 180 degrees with respect to the magnetic field. The hyperfine structure of the ions can be observed in the change of this asymmetry as a function of the Doppler-tuned optical excitation frequency.

For the purpose of β-NMR measurements [9, 10], the frequency is tuned to the strongest hyperfine component and the polarisation is destroyed by transitions between different nuclear Zeeman levels caused by irradiation with a tunable radio frequency. In a cubic host crystal the nuclear magnetic resonance takes place when the radio frequency corresponds to the Larmor frequency (ν_L) of the implanted nucleus. This frequency allows the determination of the nuclear g-factor, since $\nu_L = g\mu_N B/h$ (with B as the external magnetic field). A precise g-factor measurement requires high asymmetries and narrow resonances. Both the linewidth and amplitude of the observed resonance can depend strongly on the used

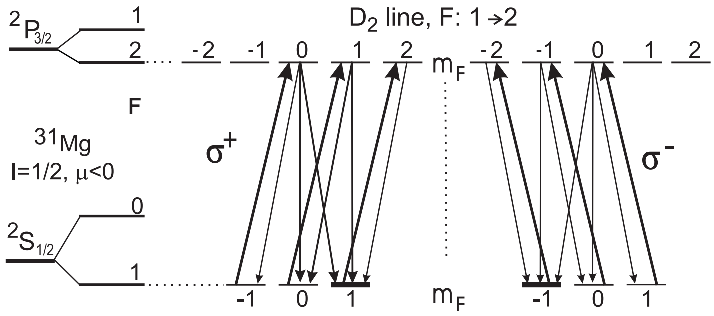

FIG. 2: Optical pumping of ^{31}Mg with an assumed spin $I = 1/2$ and a negative magnetic moment. The process is shown for $F = 1 \rightarrow F' = 2$ transitions with positive and negative laser light polarisation, which populate different m_F sublevels.

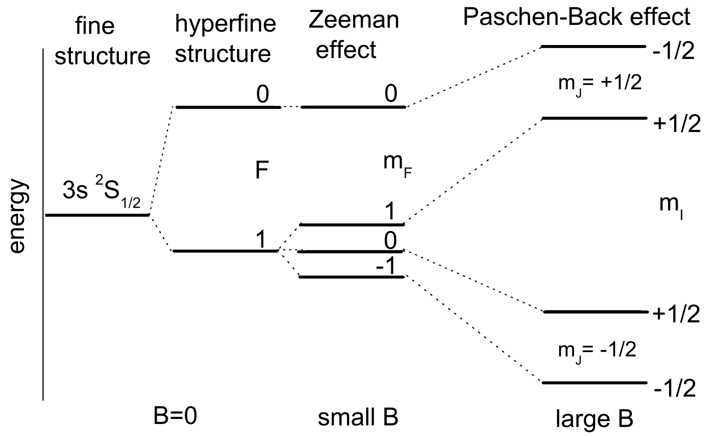

FIG. 3: Behaviour of the ground state hyperfine structure of ^{31}Mg for weak and strong magnetic field ($I = 1/2$ and negative μ assumed).

implantation crystal. Three cubic crystals were tested. At room temperature MgO turned out to be superior to metal hosts (it gave up to 6.7% asymmetry, compared to 3.1% for Pt and 1.8% for Au, all values taken for ^{31}Mg, with the linewidths comparable for all three crystals) and was therefore used for further measurements.

3 HYPERFINE STRUCTURE AND g-FACTOR OF ^{31}MG

The transitions suitable for optical pumping of Mg ions are the excitations from the ground state to the two lowest lying excited states, $3s\ ^2S_{1/2} \rightarrow 3p\ ^2P_{1/2}$ and $3p\ ^2P_{3/2}$ (D_1 and D_2 lines). The wavelength (280 nm) is in the ultraviolet range. For better efficiency (about 5%) an external cavity was used to frequency double the 560 nm output of a ring dye laser (Pyrromethene 556 as active medium), which was in turn pumped by a multiline Ar^+ laser. The UV powers obtained in this way (about 15 mW) suffice to saturate the transitions

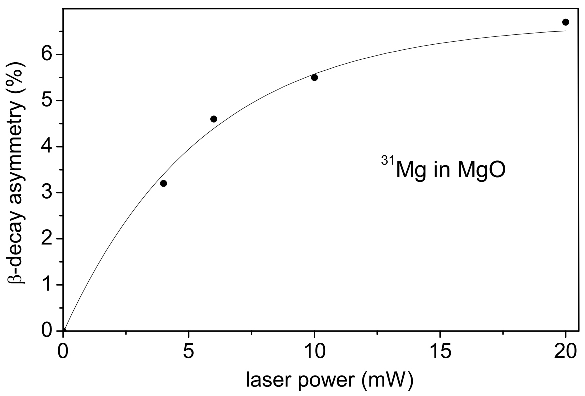

FIG. 4: β-decay asymmetry as a function of the laser power.

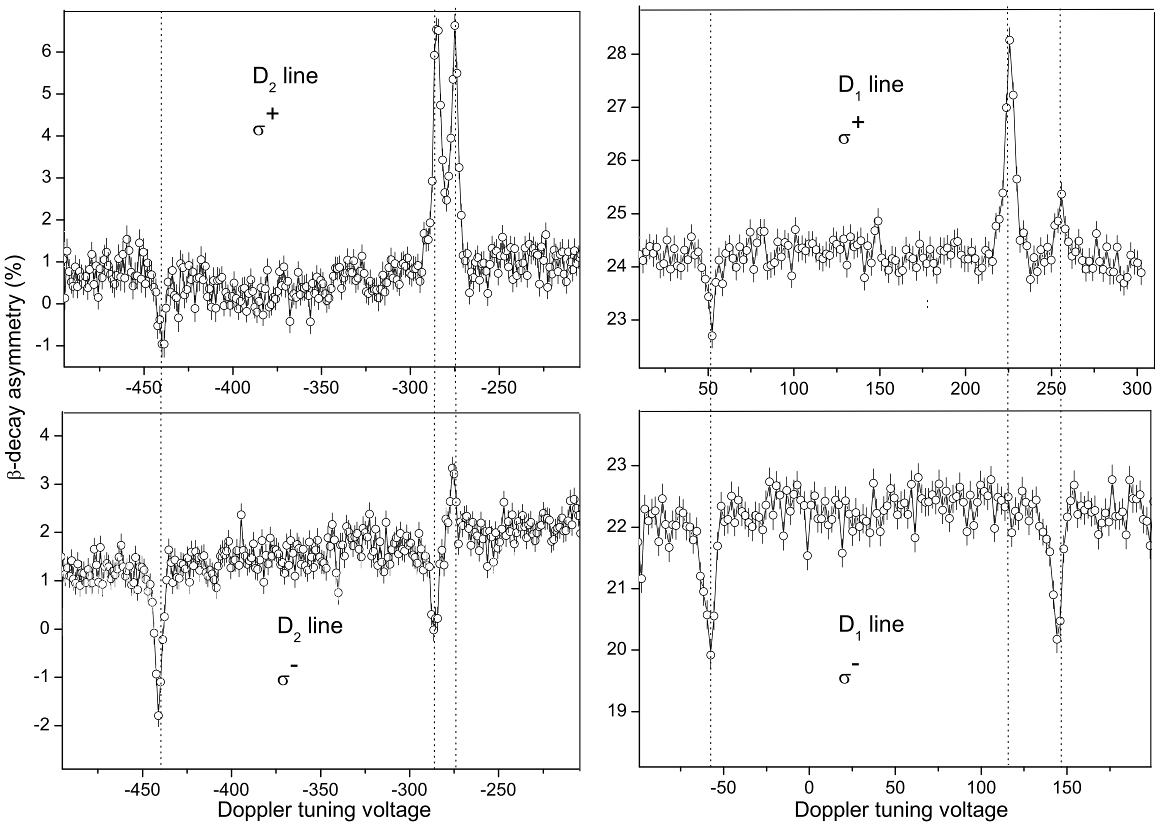

FIG. 5: Measured hyperfine structure of ^{31}Mg D_1 and D_2 lines for σ^+ and σ^- polarised light. The experimental count rate asymmetry is shown as a function of the Doppler tuning voltage.

(Fig. 4). With this setup the hyperfine structure of ^{31}Mg for both lines was recorded for σ^+ and σ^- polarised light (Fig. 5). The structures reveal 1/2 as the most probable nuclear spin, since this is the only case which can reproduce the observed three hyperfine components for both D_1 and D_2 lines, as shown in Fig. 6. For all other spins (e.g. 3/2, 7/2) there should be 4 components in the D_1 line (fully resolved) and 6 in the D_2 line (at least partly resolved).

The positive and negative resonances in Fig. 5 reflect the sign of polarisation achieved

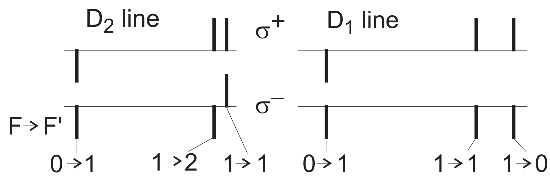

FIG. 6: Predicted hyperfine structure of ^{31}Mg D_1 and D_2 lines for $I = 1/2$ and a negative magnetic moment.

by optical pumping on the different hyperfine structure components for which only one example is shown in Fig. 2. For a quantitative explanation one has to take into account also the decay from the excited state to the other ground state level (with $F = 0$ in the case of Fig. 2). The distribution of population over the different $|F, m_F\rangle$ levels can be calculated [3] by solving rate equations including the relative transition probabilities for the excitations $|F, m_F\rangle \rightarrow |F', m_F{}'\rangle$ and subsequent decays $|F', m_F{}'\rangle \rightarrow |F, m_F\rangle$. Fig. 3 shows the rearrangement of electronic and nuclear spins by the adiabatic decoupling which occurs while the ions enter the strong magnetic field region. Apparently, the effect of σ^+ and σ^- optical pumping is asymmetric in the final population of $|m_J, m_I\rangle$ levels reached in the Paschen-Back regime. Only the distribution over the nuclear Zeeman levels m_I is responsible for the β-asymmetry signals observed in the spectra. These are different in amplitude and only partly in sign under reversal of the polarization from σ^+ to σ^- light.

After hyperfine structure scans, the acceleration voltage is fixed to the hyperfine component giving largest asymmetry (6.7% for D_2 line with σ^+) and β-NMR measurements follow. Several resonances in a cubic MgO lattice give the Larmor frequency $\nu_L(^{31}\text{Mg})=$ 3859.72(13) kHz. For the calibration of the magnetic field (within 48 hours of taking the data for ^{31}Mg) a search for Larmor resonances in the same crystal was performed on optically polarised ^{8}Li with the g-factor $g(^8\text{Li})= 0.826780(9)$ [11]. This nucleus is available from the same ISOLDE target and requires changes in the optical pumping laser system (excitation wavelength around 670 nm), as well as minor modifications to the setup. The reference Larmor frequency is $\nu_L(^8\text{Li}) = 1807.03(2)$ kHz. From the above, the deduced absolute value of the g-factor of ^{31}Mg is $|g(^{31}\text{Mg})|= 1.7671(2)$ (corrected for diamagnetism) [12]. The final error includes a systematic uncertainty accounting for the inhomogeneities of the magnetic field and its drift between the measurements on ^{31}Mg and ^{8}Li.

4 NUCLEAR MAGNETIC MOMENT AND SPIN OF ^{31}MG

The hyperfine splitting depends both on the nuclear spin and the g-factor, *e.g.* the splitting between the ground state hyperfine components of ^{31}Mg (the electronic spin $J = 1/2$) equals $\Delta\nu = A(I + 1/2)$, with the hyperfine constant $A = gH_e/J$. Based on the measured g-factor and the hyperfine splitting one can thus determine the spin and the absolute value of the magnetic moment ($\mu = gI\mu_N$) of ^{31}Mg. A reference measurement on a different Mg isotope with a known g-factor is also required, in order to calibrate for the magnetic field created by electrons at the site of the nucleus (H_e). $\Delta\nu$ can be then expressed as $\Delta\nu = A_{ref}/g_{ref} \cdot g(I + 1/2)$. For this purpose stable ^{25}Mg was chosen and was studied by means of classical collinear laser spectroscopy with the optical detection method (Fig. **??**). To verify if our measurements are performed in the correct way, we scanned the hyperfine structure of this isotope in the D_1 line (Fig. 7). The measured hyperfine structure constant for the ground state $A_{gs}(^{25}\text{Mg}) = -596.4(3)$ MHz is in excellent agreement with the accurate value quoted in the literature $-596.254376(54)$ MHz [13]. This value, together with the known magnetic moment $\mu = -0.34218(3)\mu_N$ and spin $I = 5/2$ [11] of ^{25}Mg, as well as the measured value of the ground state splitting of ^{31}Mg $\Delta\nu = 3070(50)$ MHz, reveals the spin $I = 1/2$ for ^{31}Mg. This was expected from the number of hyperfine structure components. From the positions of the resonances also the sign of the magnetic moment can be deduced ($\mu < 0$). The negative value of the magnetic moment implies furthermore a positive parity of this state. It follows both from the earlier β-decay studies [5], as well as from the large scale shell model calculations presented in Neyens et al. [12]. Calculations with different interactions, both in the sd and in the extended $sd - pf$ model spaces, predict a positive magnetic moment for the lowest $1/2^-$ state. Thus our observed negative sign excludes the negative parity option, in agreement with the assignment based on the β-decay. Therefore we conclude that $\mu(^{31}\text{Mg}) = -0.88355(10)\ \mu_N$ and $I^\pi(^{31}\text{Mg}) = 1/2^+$.

Shell model calculations in the sd model space using the USD interaction [14] predict the lowest $I = 1/2^+$ level only at 2.5 MeV excitation energy. More advanced large scale shell model calculations, including excitations of neutrons into the pf-shell, and using the interactions as described in [15] and in [16], both predict the $1/2^+$ level below 500 keV and with a magnetic moment close to our observed value [12]. The wave function of this $1/2^+$ state consists mainly of intruder configurations, which places this nucleus inside the "island of inversion".

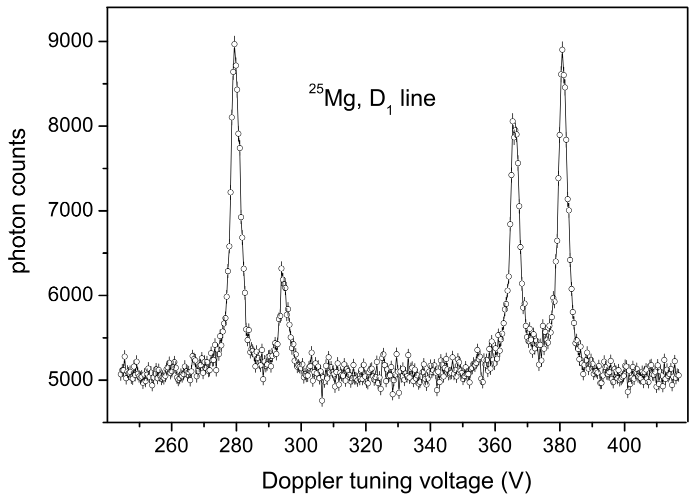

FIG. 7: Hyperfine structure of $^{25}Mg^{+}$ recorded by detecting the photons emitted during the relaxation of the ions in the optical detection part of the setup.

This unambiguous spin-parity measurement allowed us also to make tentative assignments to the lowest lying excited states in ^{31}Mg [12].

Similar measurements have also been performed for ^{29}Mg. They include the nuclear g-factor and the ground state spin $I = 3/2$, which is well described in the *sd* shell model. This measurement places the ground state of ^{29}Mg outside the "island of inversion". Study of shorter-lived ^{33}Mg is planned for the future.

This work has been supported by the German Ministry for Education and Research (BMBF) under contract No. 06MZ175, by the IUAP project No. p5-07 of OSCT Belgium and by the FWO-Vlaanderen, by Grant-in-Aid for Specially Promoted Research (13002001).

[1] C. Thibault *et al.*, Phys. Rev. C **12**, 644 (1975).
[2] C. Detraz *et al.*, Phys. Rev. C **19**, 164 (1979).
[3] M. Keim *et al.*, Eur.Phys. J. A **8**, 31 (2000).
[4] D. Guillemaud-Mueller *et al.*, Nucl. Phys. A **426**, 37 (1984).
[5] G. Klotz *et al.*, Phys. Rev. C **47**, 2502 (1993).
[6] S. Nummela *et al.*, Phys. Rev. C **64**, 054313 (2001).
[7] U. Köster *et al.*, Nucl. Instr. Meth. B **204**, 347 (2003).
[8] R. Neugart *et al.*, Nucl. Inst. Meth. **186**, 165 (1981).
[9] W. Geithner *et al.*, Phys. Rev. Lett. **83**, 3792 (1999).
[10] E. Arnold *et al.*, Phys. Lett. B **197**, 311 (1987).
[11] P. Raghavan, At. Data Nucl. Data Tables **42**, 189 (1989).
[12] G. Neyens *et al.*, Phys. Rev. Lett. **94**, 22501 (2005).
[13] W.M. Itano, D.J. Wineland, Phys. Rev. A **24**, 1364 (1981).
[14] B.H. Wildenthal *et al.*, Phys. Rev. C **28**, 1343 (1983).
[15] S. Nummela *et al.*, Phys. Rev. C **63**, 44316 (2001).
[16] Y. Utsuno *et al.*, Phys. Rev. C **64**, 11301 (2001).